

PREDICTION OF MECHANICAL PROPERTIES OF DIRECT METAL LASER SINTERED 15-5PH STEEL PARTS USING BAYESIAN INFERENCE – A PRELIMINARY STUDY

Ala Qattawi
University of California, Merced
Merced, CA

Durul Ulutan¹
California State University, Northridge
Northridge, CA

Ala'aldin Alafaghani
University of California, Merced
Merced, CA

ABSTRACT

Direct Metal Laser Sintering (DMLS) is an additive manufacturing process where metal parts are created layer by layer. Mechanical properties of the final product can vary significantly based on processing parameters. In traditional processes, such effects of processing parameters on mechanical properties are well-established. However, additive manufacturing methods are relatively new, which means there is less consensus, if at all, on how processing parameters affect mechanical properties of the final product. This study is a preliminary effort toward understanding the effects of processing parameters on mechanical properties of the metal. Processing parameters studied were the fabrication direction and temperature. Mechanical properties that were studied were the yield and tensile strength of the built material. 15-5PH stainless steel parts were DMLS fabricated with varying temperatures and directions for this purpose and their mechanical properties were measured. Then, a statistical approach was followed in order to generate a probabilistic prediction model. In this approach, Gibbs sampling was used to randomly sample from population of coefficients, Metropolis algorithm was used for decision-making purposes based on performance of different coefficient sets, and an empirical model was hypothesized. Then, the model was trained using a training dataset, and the cloud of coefficient sets for the hypothesized equation were obtained. Using these coefficient sets, the probable normal distribution of other test conditions was predicted and verified using testing data. It was shown that all measurements were well within the confidence interval of predictions, with a maximum difference of 4% between mean predictions and measurements. It was also observed that with a coefficient of variation smaller than 18%,

spread of predictions was low enough to suggest that predictions were precise as well as their accuracy.

Keywords: Direct Metal Laser Sintering, Bayesian Inference, Gibbs sampler, 15-5PH steel.

INTRODUCTION

Direct Metal Laser Sintering (DMLS) process is a type of additive manufacturing used to create metal parts layer by layer. Due to the many processing parameters involved in the DMLS process [1], produced parts are subjected to high variability in terms of expected performance and mechanical properties. This knowledge is well-established for traditionally manufacturing processes and knowledge in the field as Design-for-Manufacturing (DFM), so after investigating the effect of a certain set of manufacturing processes parameters, resulting design can be finalized. A general design guideline is created to avoid defects, and the part is designed for easy manufacturability considering the capabilities of the chosen manufacturing process.

In additive manufacturing (AM), however, these guidelines are still under consideration since the effect of each DMLS processing parameter and the interaction effects of a set of processing parameters are still under investigation. Particularly, effect of DMLS processing parameters on mechanical properties of produced parts is an unknown territory [2-5]. Researchers work on identifying mechanical properties, and they have already established that with the current DMLS capabilities, mechanical properties of DMLS parts can be less favorable than traditionally manufactured metal parts [6-8]. Focus of such research has been on high strength-to-weight ratio metals such

¹ Contact author: durul.ulutan@csun.edu

as 15-5 PH stainless steel, as well as titanium and nickel-based alloys [9-10].

Several uncontrollable factors affect resulted part quality in DMLS, such as melting pool dynamics, presence of voids, heating zone inconsistency, and varying size of metal powder particles [11-12]. These factors can lead to variation in DMLS mechanical properties and uncertainty in property prediction models. Researcher developed simulation models to predict the temperature field, melt pool and thermal history in the heat affected zone taking into consideration processing parameters such as laser power and diameter, laser scanning speed, scanning style, and layer thickness [13-15]. This helps in predicting the developed microstructure, mechanical properties and surface roughness [16-19]. However, simulating laser sintering process has proven to be complicated and computationally demanding. Therefore, approximations and assumptions are necessary to reduce the computational power required [20-21]. This leads the results of simulations to be less accurate. Some researchers used empirical and regression models instead [22-25]. However, most designs of experiments require a large number of runs to capture parameter interactions and noise [26-27], which is not feasible for metal AM due to high cost. On the other hand, researchers are able to utilize Markov Chain Monte Carlo (MCMC) simulations in modelling systems with limited number of experimental runs and include uncertainty in the analysis. MCMC has been used to create and calibrate thermal prediction models for AM [28].

To address these challenges, a probabilistic Bayesian approach using MCMC method has been used in this work. This method is a powerful tool for parameter inference and quantification of embedded uncertainties of models.

EXPERIMENTAL METHODOLOGY

To experimentally evaluate the effect of elevated environmental temperatures and building orientation on the mechanical properties of DMLS 15-5PH steel parts, DMLS specimens were fabricated in three different orientations and then tested at three different environmental temperatures. A total of 9 patches were fabricated. Each patch contained two specimens to check the repeatability. Every three patches were fabricated in one of the three principal orientations XYZ, YZX, ZXY described in ASTM-F2971-13 standards [29] and abbreviated in this work as X, Y, and Z, respectively as shown in Fig. 1. Three patches, one X, one Y and one Z, were tested at room temperature. Another three patches were tested at 200°C and the last three were tested at 350°C. Therefore, for each testing temperature, all three different orientations were investigated. Specimen numbers, assigned building direction, and the testing temperature, as well as the experimental results showing the yield and tensile strength of the fabricated parts are listed in Table 1.

All the 15-5PH steel specimens were fabricated on EOSINT M 270 system using PH1 metal powder from EOS. Chemical composition by weight percentage of the raw powder used to fabricate specimens are listed on Table 2. Processing parameters used during additive manufacturing of the specimens such as

laser power and layer thickness are listed in Table 3. Specimens were fabricated according to ASTM-E8/E8M [30]. The shape and dimensions of the specimens are shown on Fig. 2 for the reader's convenience.

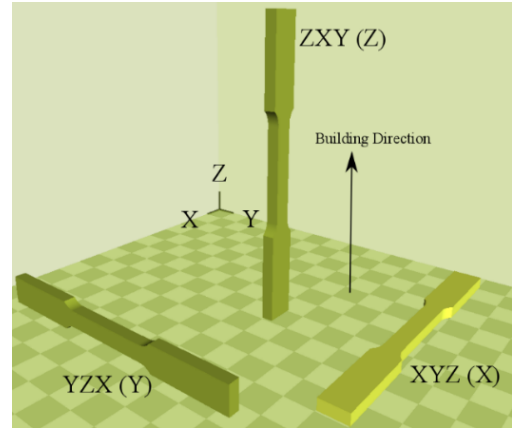


FIGURE 1: THREE ORIENTATIONS USED IN FABRICATING THE SPECIMENS

The tensile tests were performed using an Instron universal testing machine 3369 with an environmental chamber with a type N thermocouple. The tests were done according to ASTM E8/E8M and E21 [31] standards for axial tension tests of metallic specimens with elevated temperature. The tests started after 30 minutes minimum of reaching the testing temperature to ensure thermal equilibrium. A strain rate of 0.005/min before yield was achieved using an extension rate of 0.16 mm/min per the ASTM E21 standards. The data collected were time, extension, load, and the strain recorded by a high-temperature extensometer with 25 mm gauge length.

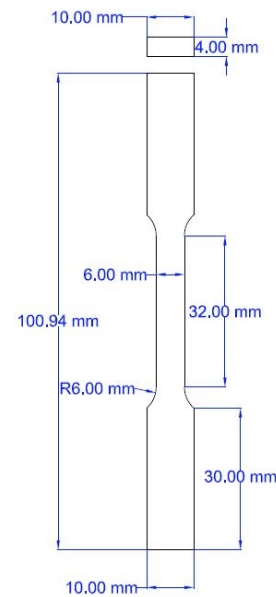


FIGURE 2: DIMENSIONS OF FABRICATED SPECIMENS

TABLE 1: SAMPLE SPECIFICATIONS & EXPERIMENTAL RESULTS

Test No.	Build Direction	Test T [°C]	Yield Strength [MPa]	Tensile Strength [MPa]
1	X	20	1024	1168
2	X	20	1008	1148
3	Y	20	1006	1158
4	Y	20	990	1146
5	Z	20	957	1158
6	Z	20	947	1159
7	X	200	946	1019
8	X	200	925	1021
9	Y	200	897	1036
10	Y	200	916	1027
11	Z	200	919	1006
12	Z	200	928	993
13	X	350	878	1003
14	X	350	808	1028
15	Y	350	860	1017
16	Y	350	841	997
17	Z	350	877	1004
18	Z	350	886	1003

THEORY

The statistical theory used in this study was inherited from [32], but for the convenience of the author, it will be reiterated here. Application of the theory and the methodology is similar; however, since the data comes from a completely different process, results are not reproduction of the previous study. Application of this method to prediction of outputs is not novel. However, predicting additive manufacturing outputs with the accuracy achieved using this method underlines the novelty of this study. This method is particularly useful when there is a scarcity of data points and accurate predictions from such data is still expected. In this section, the method is explained in detail, and results of the method applied on experimental data is presented in the next section.

3.1 Bayes Rule

Bayes rule is explained best with an example: Assume that you are provided with two bags full of balls, and you were told that bag #1 has four red balls and one green ball, whereas bag #2 has three green balls and two red balls. If you are to pick a ball randomly from one bag but you do not have information on bag numbers or contents, probability of picking a red ball would be 0.6 (60%). This is called “prior probability,” or an “*a priori*” knowledge (initial belief) of the event that is “picking a red ball.”

Now suppose that you are provided with labeled bags and their contents. Then, based on direct logic, you would want to pick from bag #1 to increase your chances of picking a red ball. This is because you have 0.8 (80%) probability to pick a red ball from bag #1 whereas you have 0.4 (40%) probability of the same

event with bag #2. Therefore, you are making a decision based on the “posterior probability” of the event – an “*a posteriori*” (informed) decision. In this scenario, if we call the choice of bag #1 event X , and the picking of a red ball event Y , then $p(y)$ is the *a priori* probability distribution of picking the red ball, and $p(y|x)$ is the *a posteriori* probability distribution based on information gathered from event X . The relationship between two probabilities are given by the Bayes rule as shown in Eq. (1). In this equation, $p(x)$ is the probability distribution of event X . Without any other information provided, the choice of bag would be completely random, so in our problem, $p(x) = 0.5$. More importantly, regardless of the complexity of the problem, this number is generally assumed to be constant, and instead of the equality, a proportionality is used as shown in Eq. (2). The last term, $p(x|y)$ is the conditional probability of X . In our problem, that would be the probability of having chosen bag #1 if a red ball is known to be picked. Imagine a scenario when you do not have labels again and you randomly pick a ball from one of the bags. If the ball you picked is a red ball, what is the probability that the bag you picked from was bag #1? This is called the conditional probability of X given the information Y .

Most of the times, it is almost impossible to come up with the conditional probability of X given Y . In such cases, one can approximate the conditional probability to the multiplication of individual observations, so $p(X|y) = p(x_1, \dots, x_n|y)$, resulting in Eq. (2).

$$p(y|x) = \frac{p(x|y)p(y)}{p(x)} \quad (1)$$

$$p(y|x) \propto p(X|y)p(y) \quad (2)$$

3.2 Gibbs Sampler

In order to get $p(X|y)$, one needs to sample from the population. There are many different methods to sample from a population, and Gibbs sampler is an MCMC algorithm where a utilization function that is dependent on the inputs and unknown coefficients is used. To illustrate, in order for Gibbs sampler to work, one needs a model as shown in Eq. (3). In such a model, Y is the set of observations, X is the set of conditions (inputs), K is the set of coefficients to be determined, and ε is the measurement error of the observations. This error is assumed to be normally distributed with zero mean and σ standard deviation, so $\varepsilon \sim N(0, V)$, where $V = \sigma^2$.

$$Y = f(X, K) + \varepsilon \quad (3)$$

Therefore, once you have the observations (data set), the only unknowns of the equation are the K_i and V . If one can get the “*a posteriori*” joint probability density function of the unknowns, Gibbs sampler is said to be completed. This density function is given on the left hand side of in Eq. (4), where $p(K|V, X, Y)$ is the full conditional of the coefficient set K , and $p(V|X, Y)$ is the marginal distribution of V .

$$p(K, V|X, Y) \propto p(K|V, X, Y)p(V|X, Y) \quad (4)$$

TABLE 1: CHEMICAL COMPOSITION BY WEIGHT PERCENTAGE OF THE RAW POWDERS USED TO FABRICATE DMLS SPECIMENS

15-5PH	Cr	Ni	Cu	Mn	Si	C	Mo	Nb	Fe
	14.0-15.5	3.5-5.5	2.5-4.5	1.00 max	1.00 max	0.07 max	0.5 max	0.15-0.45	Bal

TABLE 2: DMLS PROCESSING PARAMETERS USED WHILE FABRICATING THE SPECIMENS

Metal	System	Laser Power	Laser Diameter	Scan Style	Layer Thickness	Inert Gas
15-5PH	M 270	200 W	100 microns	Alternating Stripes	40 microns	N2

Then, in order to get the “*a posteriori*” joint probability density function, one needs to find the full conditional of K and the marginal distribution of V . The full conditional of K can be written as shown in Eq. (5) using Bayes rule, where the first term is the conditional probability distribution of the observations, which is just a multiplier. The second term is the *a posteriori* probability distribution of coefficient set, which is equivalent to the *a priori* probability distribution of the coefficient set ($p(K | V, X) = p(K)$) since the coefficient set is independent of the error variance and the observation inputs. Therefore, Eq. (6) can be derived, since the coefficients can be assumed to be of normal distribution with a mean vector μ_K and covariance matrix Σ_n , where the mean vector and covariance matrix can be found using Eq. (7) and Eq. (8). In these equations, K_0 and Σ_n are the initial assumptions of the coefficient vector and the covariance matrix. Therefore, choosing the initial assumption of K_0 to be equal to a set of zeros or ones and the initial assumption of the covariance matrix to be equal to the identity matrix make the calculations significantly easier. There is not a big issue with the assumption of no covariance between coefficients (matrix is identity). However, assigning K_0 an arbitrary set of numbers increases the risk of divergence. Similar to any search algorithm, Gibbs sampler also has the inherent risks of divergence and local minima. Therefore, it is essential to start with a set of coefficients that is meaningful. Using an optimization algorithm to find a good-enough initial assumption for coefficients increases the speed, convergence rate, and the success rate of the search algorithm.

$$p(K | V, X, Y) \propto p(Y | K, V, X) p(K | V, X) \quad (5)$$

$$p(K | V, X, Y) \propto N(\mu_K, \Sigma_n) \quad (6)$$

$$\mu_K = \Sigma_n \left(\Sigma_0^{-1} K_0 + \frac{X^T Y}{V} \right) \quad (7)$$

$$\Sigma_n = \left(\Sigma_0^{-1} + \frac{X^T X}{V} \right)^{-1} \quad (8)$$

Once the first term in Eq. (4) is found using Eq. (5) through Eq. (8), the second term that is the marginal distribution of V also needs to be found. Hoff showed that the *a priori* distribution of variance can be approximated as an inverse-gamma distribution with parameters $n/2$ and $n^*V_0/2$, where v_0 is the sample size and V_0 is the sample variance [33]. Using Eq. (9), one can see that the marginal distribution of V is directly proportional to its *a*

priori distribution, since it is directly proportional to its a posteriori distribution, which is equivalent due to the fact that the variance is independent of the inputs. Therefore, the marginal distribution of V also follows an inverse-gamma distribution.

$$\begin{aligned} p(V | X, Y) &\propto p(Y | V, X) p(V | X) \propto p(V), \\ p(V) &\propto IG\left(\frac{n}{2}, \frac{nV_0}{2}\right) \end{aligned} \quad (9)$$

Moreover, since the sum of squared errors for each set of coefficients is $SSE = \sum_{i=1}^N [Y - f(X, K)]^2$, where N is the number of observations, the conditional probability distribution of the observations acts as a shifting parameter in the inverse-gamma distribution. When multiplied, the marginal distribution of V can be obtained from Eq. (10).

$$p(V | X, Y) \propto IG\left(\frac{n+N}{2}, \frac{nV_0+SSE}{2}\right) \quad (10)$$

As a result, using the initial assumption of the coefficient set and the covariance matrix, input data, output data, and variance of the error, full conditional of the coefficient set can be obtained. In order to do that, variance of the error needs to be calculated first, which can be done by creating a random number based on an inverse-gamma distribution with the parameters shown on Eq. (10). Therefore, at each step, a new set of coefficients can be generated using the Gibbs sampler algorithm, based on the previous coefficient set (since previous set of coefficients is used to calculate SSE), set of initial assumptions, and the data.

3.3 Metropolis Algorithm

Gibbs sampler is a quick and easy method to sample from the population when an insufficient dataset is available. However, the user cannot decide on whether or not the coefficient set obtained using the Gibbs sampler is appropriate without a selection algorithm. This is why the Metropolis algorithm is employed in this study. In this algorithm, a new choice of a candidate solution is generated at each iteration, and this candidate solution is compared to the last accepted solution. If the candidate solution has a comparable performance to the last accepted solution, then it is accepted and added to the cloud of acceptable solutions. If not, the candidate solution is rejected and a new iteration starts.

To start a new iteration, a sample K^k is drawn from the full condition of K , using the normal distribution shown in Eq. (6) achieved with Gibbs sampler. This solution is used to calculate

SSE for the current iteration, which leads to finding variance V_k of current iteration. Then, this variance is passed into the Metropolis algorithm, along with the set of coefficients of the current iteration K^k . Then, a candidate new solution K^* is generated using $K^* = K^k + q^k$, where $q^k \sim N(0, \delta^2)$. Selection of variance δ^2 is critical, as it plays an important role in determining convergence. If it is selected too small, algorithm may not converge within given amount of time and iterations or may not be able to get out of a local minimum. If it is selected too big, jerky movements of the coefficient set between iterations may be possible, and this may again cause divergence due to oscillating solutions. In addition, big selection of the variance δ^2 might cause an increased rejection rate, which makes the algorithm inefficient. More involved solutions such as the Jacobian matrix solution can be utilized in determining what the variance should be; however, all inputs and outputs must be normalized if the Jacobian is used to avoid singularity issues, particularly with increased number of coefficients [34]. In this study, since the number of coefficients used is high, to avoid potential convergence issues, a constant variance of $\delta^2 = 1$ was used.

Once the candidate new solution is generated, its performance needs to be measured and compared against the performance of the previous solution. In order to do that, the full conditional of the candidate solution K^* is calculated and compared to the full conditional of the previous solution using Eq. (11). The ratio between the two performances (probabilities) is denoted with r , and it can virtually take any value in the range of $[0, \infty]$. Then, a random number U is generated between 0 and 1 using a uniform distribution. This random number is compared to the ratio r and only if $U < r$, the candidate coefficient set is accepted. Otherwise, candidate solution is rejected and the iteration counter is incremented. After a pre-determined number of iterations are completed, all of the accepted solutions are used to create a cloud of solutions.

For this method to succeed, there is a need for training data, and an independent testing data. Algorithm needs to be trained with training data to find the pseudo-optimal cloud of solutions. Then testing data is used to test the validity of the solution cloud. Since multiple solutions can be generated even with a limited number of experiments, and even replications of same tests can be treated as separate tests, this method is particularly useful when there is insufficient data to create a model. With the solution cloud created, outputs of testing data can be predicted, which will give a normal distribution due to the Central Limit Theorem. Then, a confidence interval can be determined for the prediction, which represents real situations better than a deterministic solution, since real data rarely follows a pattern to the fullest. Due to limitations with capabilities and scope of the study, part of the data that represents full data sufficiently is selected as training data and rest of the data is treated as testing data. Future work will use the whole dataset to train the model and do predictions and use a separate dataset as testing data.

3.4 Empirical Model

To be able to use the Gibbs-Metropolis algorithm described, there needs to be a model that the data is fitted to. Most of the

times, there are prior studies where approximate relationships are known. However, there is insufficient amount of effort on investigating the effects of temperature and fabrication direction on mechanical properties of DMLS parts, which makes it difficult to fit the data into a model. Therefore, the authors will propose a general model that will be able to represent any parameter and interaction effects on the outputs that can be summarized in Eq. (11). In this equation, Y represents any mechanical property, XYZ represents the fabrication direction, and T represents the fabrication temperature in Celsius. All inputs and outputs were normalized to avoid singularities with the method. Also, in assigning a value to the variable XYZ , it was assumed that X-direction will be equal to 1, Y-direction equal to 2, and Z-direction equal to 3. There is no easy way to model discrete variables such as the fabricating direction; however, when the discrete variable is an input (as opposed to an output), it is feasible to assign numerical values similar to what was done in this study.

$$Y = K_1 T^{K_2} + K_3 XYZ^{K_4} T^{K_5} + K_6 \quad (11)$$

RESULTS

In this preliminary study, tests 3-8 and 11-16 were used as training data, whereas tests 1-2, 9-10, and 17-18 were used as testing data (please see Table 1 for test numbers). This was selected so that inputs of temperature and directions are distributed equally among testing and training data. For training data, due to the small number of experiments, replications were used as separate tests. For testing data, mean of the replications were used to compare with predictions.

The algorithm was run for yield and tensile strength for this preliminary study, but it will be extended to all outputs in future work. For the coefficient set, an initial value was found by using an unconstrained, no-derivative Simplex search and optimization algorithm. Since this value is treated as an educated guess, even a local minimum solution would be a better start than a random vector. The algorithm was run for 100 times, each time updating the initial solution with mean of solutions achieved in the last run. This is done to ensure that local minima do not limit the extent of possible solutions. Each run included 10000 iterations to be able to find good possible solutions. In each run, first 20% of solutions were not included in calculations since this period is considered as the “burnout” period of the algorithm.

After the final run, coefficient set with provided values of mean and covariances were found for yield and tensile strength. K_f and Σ_f are the mean and covariance matrix of final set of coefficients, as shown on Eq. (12). Numerical values of those are provided on Eq. (13-15). Using these coefficient sets, testing data was predicted with their mean and variance as well as 95% confidence intervals. In Fig. 3, an initial coefficient set with mean = 1 and identity matrix as covariance is compared. Figure 3 shows K_i as the coefficient index, since each coefficient pair is the same way. This is a good way to compare and understand the means and covariances of the final coefficients.

$$K_{yield} \sim N(K_f, \Sigma_f) \quad (12)$$

$$K_{f,yield} = \begin{bmatrix} K_1 \\ K_2 \\ K_3 \\ K_4 \\ K_5 \\ K_6 \end{bmatrix} = \begin{bmatrix} -0.079 \\ 0.541 \\ -0.004 \\ 1.072 \\ 1.086 \\ 0.209 \end{bmatrix}, \quad K_{f,tensile} = \begin{bmatrix} K_1 \\ K_2 \\ K_3 \\ K_4 \\ K_5 \\ K_6 \end{bmatrix} = \begin{bmatrix} -1.381 \\ 0.054 \\ 0.035 \\ 0.363 \\ 2.313 \\ 0.064 \end{bmatrix} \quad (13)$$

$$\Sigma_{f,yield} = \begin{bmatrix} 0.253 & -0.121 & -0.139 & -0.068 & -0.111 & 0.013 \\ -0.121 & 0.566 & 0.141 & 0.198 & -0.012 & 0.026 \\ -0.139 & 0.141 & 0.154 & 0.09 & -0.012 & -0.001 \\ -0.068 & 0.198 & 0.09 & 0.735 & -0.015 & 0.169 \\ -0.111 & -0.012 & -0.012 & -0.015 & 0.122 & -0.014 \\ 0.013 & 0.026 & -0.001 & 0.169 & -0.014 & 0.189 \end{bmatrix} \quad (14)$$

$$\Sigma_{f,tensile} = \begin{bmatrix} 0.04 & -0.001 & -0.012 & 0.021 & -0.028 & -0.004 \\ -0.001 & 0.001 & 0.004 & 0.005 & -0.004 & -0.002 \\ -0.012 & 0.004 & 0.024 & 0.016 & -0.013 & -0.007 \\ 0.021 & 0.005 & 0.016 & 0.119 & -0.04 & -0.02 \\ -0.028 & -0.004 & -0.013 & -0.04 & 0.041 & 0.011 \\ -0.004 & -0.002 & -0.007 & -0.02 & 0.011 & 0.031 \end{bmatrix} \quad (15)$$

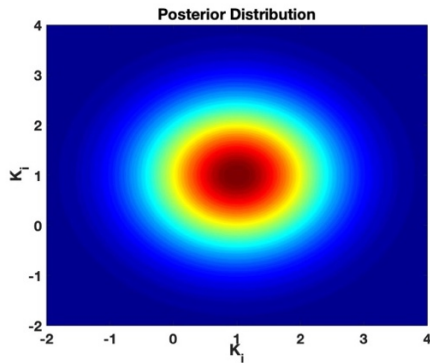


FIGURE 3: DEFAULT DISTRIBUTION OF PARAMETERS

Pairwise distributions of coefficients are provided in Fig. 4 and Fig. 5, respectively for yield and tensile strength simulations. For yield strength simulations, variance of K_1 , K_2 , and K_4 were considerably larger than the other three coefficients. In addition, mean for K_3 was sufficiently close to zero, which means that it might be wise to eliminate those coefficients (equate to zero) from the model. Obviously, if one does that, the second term in the equation vanishes completely, and yield strength becomes completely independent of the direction of fabrication. It can be observed from the dataset that this is not too distant from what data indicates, since there are minute changes with yield strength with the change in fabricating direction. Therefore, it might be a good direction in future work to eliminate that term from the model and run simulations accordingly, only with the remaining three coefficients. Another direction for future studies would be to normalize the coefficients, since there is more than an order of magnitude difference between them. When such a difference exists, the difference between parameters becomes less obvious and singularity issues may arise.

For tensile strength simulations, coefficients involved significantly less variance as well as covariance. This indicates that there is a better pattern with the value of tensile strength based on direction and temperature of fabrication. Mean values of K_2 , K_3 , and K_6 are close to zero; however, it is not possible to eliminate any of those coefficients from the model since they are also similar to one another. Value of K_1 is significantly negative,

which means that there is an inverse relationship between fabrication temperature and tensile strength of material. This is also observable from the data, which supports findings. Value of K_5 then becomes significantly positive; however, that is mainly due to K_2 being close to zero and K_1 significantly negative, so K_5 needs to pull value of output back towards normalized value.

As a result of these findings, testing data shown on Table 4 is predicted. Predictions are shown on Fig. 6 and Fig. 7, where coefficient sets found with training data were utilized separately for yield and tensile strength, respectively. In these figures, blue curves represent normal distribution of predictions with the coefficients found using training data, green vertical lines show the location of 95% confidence interval for predictions, and red lines show measurement values for testing data. These results are also presented on Table 4. All predictions align with the measurements within confidence intervals. In fact, mean value of predictions actually align very well with measurements, as shown on Table 4. For yield strength, mean value of predictions were at most 4% away from measurements, whereas confidence intervals well-covered measurement data. For tensile strength, mean value of predictions were not even 1% away from measurements, which shows outstanding success of the model. In addition, coefficient of variation c_v , which is the ratio of standard deviation to mean, was calculated in percentage and shown on Table 4 for each prediction. This shows the spread of each prediction. If this spread is high, it means there is not enough confidence in predictions. However, as shown on Table 4, for yield strength data, ratio was between 7 to 18%, which can be regarded as small spread of predicted value. Combined with the <4% error between mean prediction and measurements, it can be concluded that the algorithm worked successfully and was able to locate a good solution to predict yield strength. Similarly, for tensile strength data, the ratio (c_v) was between 1-2%, which shows excellent confidence in predictions. Combined with <1% error between mean predictions and measurements, it can be concluded that the algorithm was able to find an exceptionally well solution to predict material's tensile strength. Still, future work will utilize the whole current dataset as training data and a new set of experiments at different temperatures as testing data, to ensure independence of testing and training data.

At the end, the reader may question the rationale for employing a rather complex algorithm to achieve results that seem relatively straightforward to achieve using standard curve fitting algorithms. However, a few things should be kept in mind: 1) This method is particularly useful in situations where data points are scarce, for example due to limited resources. 2) Instead of predicting a deterministic set of results, a confidence interval is achieved, which ensures that the stochastic nature of the process is represented as well. 3) Contrary to subtractive methods, accurate achievement of mechanical properties is very difficult with additive manufacturing. Therefore, predicting the results with very small coefficient of variation in addition to small errors means that predictions are strong. 4) The small coefficient of variation also indicates an increase reliability of the final product, which is important in production parts, particularly fabricated through additive methods.

TABLE 4: COMPARISON OF YIELD AND ULTIMATE STRENGTH PREDICTIONS TO MEASUREMENTS

Test	T °C	XYZ	Yield Strength				Ultimate Strength			
			Measurement MPa	Prediction MPa	Error %	c_v %	Measurement MPa	Prediction MPa	Error %	c_v %
1	20	X	1016	977 (± 175)	4	9	1158	1154 (± 40)	0.3	2
2	200	Y	907	917 (± 121)	1	7	1031	1022 (± 28)	0.8	1
3	300	Z	882	849 (± 292)	4	18	1003	996 (± 43)	0.7	2

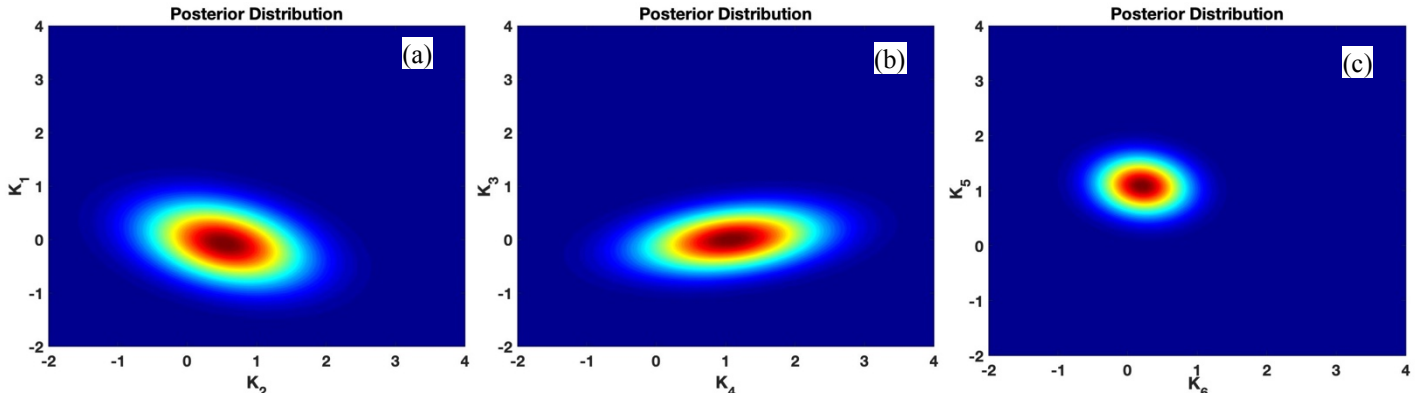


FIGURE 4: PAIRWISE DISTRIBUTION OF (A) K1 AND K2, (B) K3 AND K4, (C) K5 AND K6 FOR YIELD STRESS SIMULATIONS

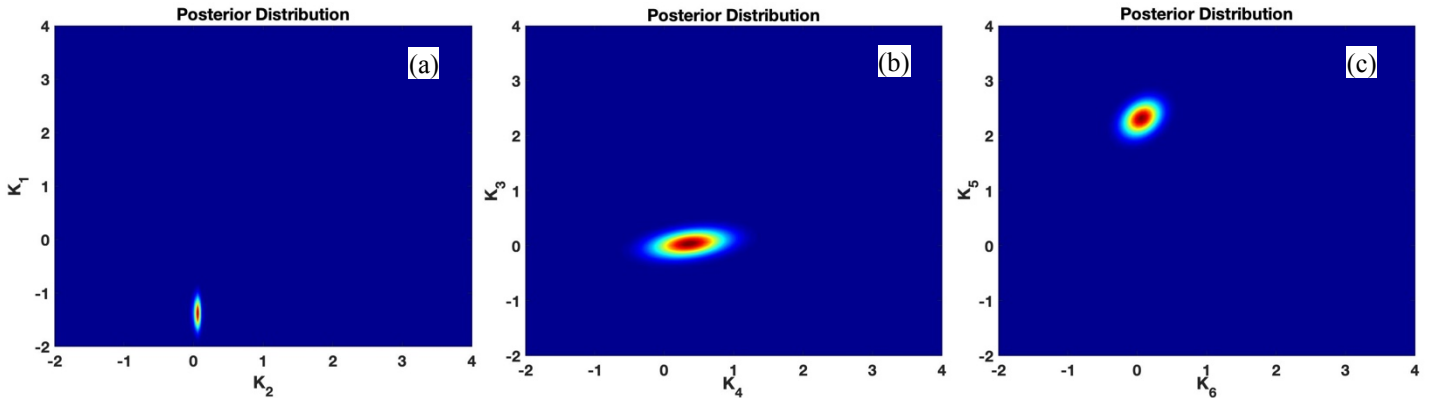


FIGURE 5: PAIRWISE DISTRIBUTION OF (A) K1 AND K2, (B) K3 AND K4, (C) K5 AND K6 FOR TENSILE STRESS SIMULATIONS

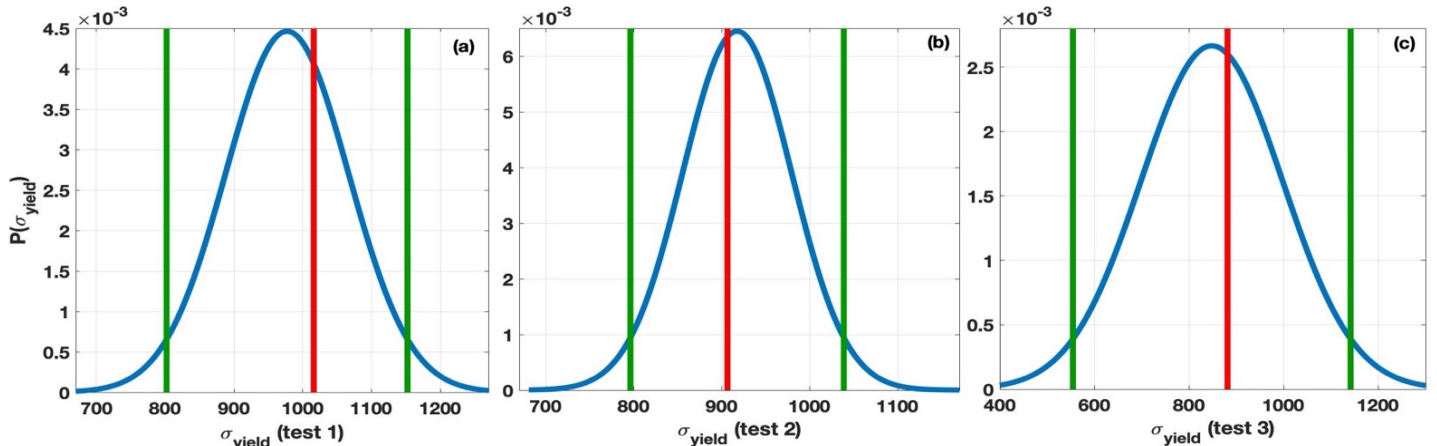


FIGURE 6: RESULTS OF THE STUDY FOR YIELD STRENGTH FOR (A) TEST 1, (B) TEST 2, (C) TEST 3 (ON TABLE 4).

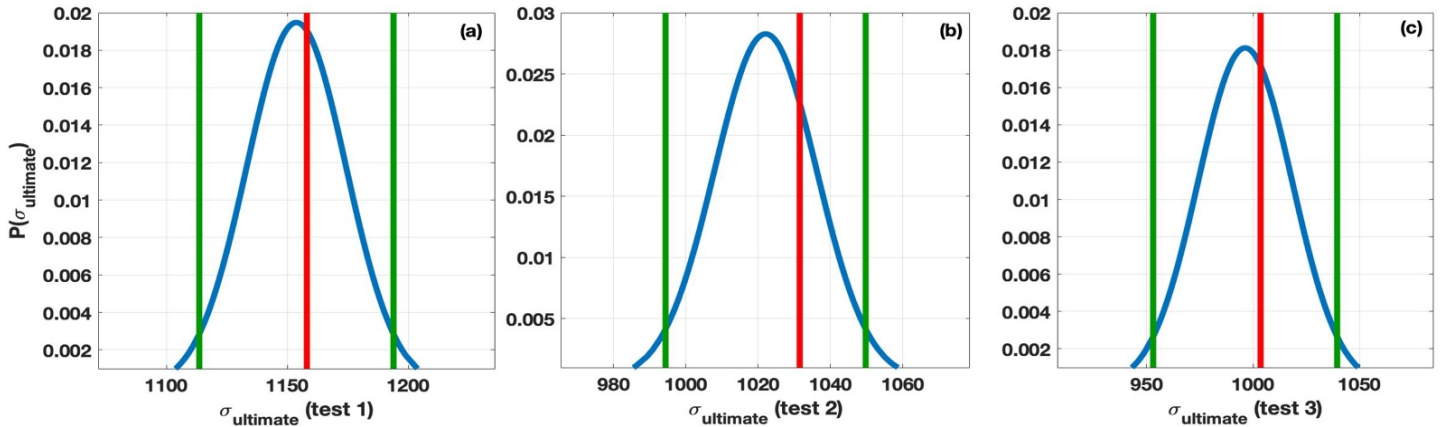


FIGURE 7: RESULTS OF THE STUDY FOR ULTIMATE STRENGTH FOR (A) TEST 1, (B) TEST 2, (C) TEST 3 (ON TABLE 4)

CONCLUSIONS AND FUTURE WORK

In this study, a statistical approach utilizing the Gibbs-Metropolis algorithm was employed in modeling the mechanical properties of DMLS parts based on their fabrication direction and temperature. The target of this preliminary study was to build the hypothesis that will eventually lead to the model and test it on a few aspects of the process. For that reason, tests with 15-5PH steel were conducted and mechanical properties of the fabricated parts were measured. Out of those properties, yield and ultimate strength of the parts were selected as the outputs to be utilized in this preliminary study. In the study, the main aim was to create a model and an algorithm that implements statistical uncertainty analysis to generate a way to predict the outputs in the lack of rich data. Based on these expectations, simulations were run, and the following conclusions were drawn out of the results:

- For both yield strength and tensile strength, mean predictions were within a few percent distance from the measurement values. This shows the high accuracy of the proposed method and the model.
- For each of the outputs, coefficient of variation (c_v) was calculated, and since this ratio was low for most of the calculations (<10%) and only 18% for one of the tests, it was concluded that there is not a huge spread in simulated values. This shows a great confidence in the location of the calculated values without the need to conduct more tests or do further replications.
- Combining the small error between the measurements and predictions and the small coefficient of variation, it can be concluded that the algorithm was successful to predict the outcomes of the process.
- Low error between predictions and experiments is not the easiest thing to achieve, but depending on conditions and with some luck, most methods can achieve it. However,

particularly if the method is deterministic, having low error between predictions and experiments does not necessarily mean that the method succeeded. Success of a method does not solely mean accurate prediction of an output with one-off measurements. Instead, its ability to predict the output of the process accurately within a confidence interval that encompasses all conditions regardless of regular environmental changes should be also sought after (continuous accuracy). Moreover, the range of the confidence interval should match the range of the possible output due to such regular and expectable changes (high precision). In this study, in addition to the predicted values of yield and tensile strength being very similar to experimental values (high accuracy), it was shown that the spread in the prediction range is narrow (precision). Finally, since additive manufacturing results are usually not as precisely predicted as more traditional processes, having high precision indicates high reliability of the tests and the product itself.

- Although it has no effect in how the results turned out, ideally training data and testing data should be collected at different times, and testing data should be collected after the model is built. Since this was a preliminary study, this requirement was ignored. However, future studies will include further testing to show the results of the algorithm in a bias-free environment.
- Furthermore, future work will include other materials such as IN-718, which have different characteristics that affect their mechanical properties differently. Moreover, algorithm will be applied to other aspects of mechanical properties such as the Young's Modulus, yield strain, and ductility of the materials. This way, it will be possible to test prediction capability of the algorithm with more models.

- Finally, the method will be improved in a future study to include a Jacobian calculation to achieve the variance of the random push instead of setting it to a single value. This increases the stochasticity of the model and therefore brings it closer to a real-life simulation.

ACKNOWLEDGEMENTS

The authors would like to acknowledge Dr. Farbod Akhavan Niaki for his contributions in application of the Gibbs-Metropolis algorithm to the experimental data.

REFERENCES

- [1] Sames, William J., List, F. A., Pannala, Sreekanth, Dehoff, Ryan R., and Babu, Sudarsanam Suresh. "The Metallurgy and Processing Science of Metal Additive Manufacturing." *International Materials Reviews* Vol. 61 No. 5 (2016): pp. 315-360.
- [2] Hu, Zhiheng, Zhu, Haihong, Zhang, Hu, and Zeng, Xiaoyang. "Experimental Investigation on Selective Laser Melting of 17-4PH Stainless Steel." *Optics & Laser Technology* Vol. 87 (2017): pp. 17–25.
- [3] Croccolo, Dario, De Agostinis, Massimiliano, Fini, Stefano, Olmi, Giorgio, Bogojevic, Nebojsa, and Ciric-Kostic, Snezana. "How Build Orientation and Thickness of Allowance May Affect the Fatigue Response of DMLS Produced 15-5 Ph Stainless Steel." *Proceedings IRF2018: 6th International Conference Integrity-Reliability-Failure*. 7214: pp. 987-996. Lisbon, Portugal, July 22-26, 2018.
- [4] Alafaghani, Ala'aldin, Qattawi, Ala, and Castañón, Mauricio Alberto Garza. "Effect of Manufacturing Parameters on the Microstructure and Mechanical Properties of Metal Laser Sintering Parts of Precipitate Hardenable Metals." *The International Journal of Advanced Manufacturing Technology* Vol. 99 No. 9-12 (2018): pp. 2491-2507.
- [5] Rashid, Rahman, Masood, Syed H., Ruan, Dong, Palanisamy, Suresh, Rashid, Rizwan Abdul Rahman, and Brandt, Milan. "Effect of Scan Strategy on Density and Metallurgical Properties of 17-4PH Parts Printed by Selective Laser Melting (SLM)." *Journal of Materials Processing Technology* Vol. 249 (2017): pp. 502–511.
- [6] Yadollahi, Aref, Shamsaei, Nima, Thompson, Scott M., Elwany, Alaa, and Bian, Linkan. "Effects of Building Orientation and Heat Treatment on Fatigue Behavior of Selective Laser Melted 17-4 PH Stainless Steel." *International Journal of Fatigue* Vol. 94 (2017): pp. 218-235.
- [7] Gratton, Alexander. "Comparison of Mechanical, Metallurgical Properties of 17-4PH Stainless Steel between Direct Metal Laser Sintering (DMLS) and Traditional Manufacturing Methods." *Proceedings of The National Conference on Undergraduate Research (NCUR2012)*. pp. 423-431. Ogden, Utah, March 29-31, 2012.
- [8] Rafi, H. Khalid, Starr, Thomas L., and Stucker, Brent E. "A Comparison of the Tensile, Fatigue, and Fracture Behavior of Ti-6Al-4V and 15-5 PH Stainless Steel Parts Made by Selective Laser Melting." *The International Journal of Advanced Manufacturing Technology* Vol. 69 No. 5–8 (2013): pp. 1299–1309.
- [9] Murr, Lawrence E., Gaytan, Sara M., Ramirez, Diana A., Martinez, Edwin, Hernandez, Jennifer, Amaton, Krista N., Shindo, Patrick W., Medina, Francisco R., and Wicker, Ryan B. "Metal Fabrication by Additive Manufacturing Using Laser and Electron Beam Melting Technologies." *Journal of Materials Science & Technology* Vol. 28 No. 1 (2012): pp. 1–14.
- [10] López-Castro, Juan D., Marchal, A., González, L., and Botana Pede, Francisco Javier. "Topological Optimization and Manufacturing by Direct Metal Laser Sintering of an Aeronautical Part in 15-5PH Stainless Steel." *Procedia Manufacturing* Vol. 13 (2017): pp. 818–824.
- [11] Mahmoudi, Mohamad, Elwany, Alaa, Yadollahi, Aref, Thompson, Scott M., Bian, Linkan, and Shamsaei, Nima. "Mechanical Properties and Microstructural Characterization of Selective Laser Melted 17-4 PH Stainless Steel." *Rapid Prototyping Journal* Vol. 23 No. 2 (2017): pp. 280–294.
- [12] Mower, Todd M., and Long, Michael J. "Mechanical Behavior of Additive Manufactured, Powder-Bed Laser-Fused Materials." *Materials Science and Engineering: A* Vol. 651 (2016): pp. 198–213.
- [13] Bontha, Srikanth, Klingbeil, Nathan W., Kobryn, Pamela A., and Fraser, Hamish L. "Thermal Process Maps for Predicting Solidification Microstructure in Laser Fabrication of Thin-Wall Structures." *Journal of Materials Processing Technology* Vol. 178 No. 1–3 (2006): pp. 135–142.
- [14] Long, Ri-Sheng, Liu, Wei-Jun, Xing, Fei, and Wang, Hua-Bing. "Numerical Simulation of Thermal Behavior during Laser Metal Deposition Shaping." *Transactions of Nonferrous Metals Society of China* Vol. 18 No. 3 (2008): pp. 691–699.
- [15] Chiumenti, Michelle, Neiva, Eric, Salsi, Emilio, Cervera, Miguel, Badia, Santiago, Moya, Joan, Chen, Zhuoer, Lee, Caroline, and Davies, Christopher. "Numerical Modelling and Experimental Validation in Selective Laser Melting." *Additive Manufacturing* Vol. 18 (2017): pp. 171–185.
- [16] Masoomi, Mohammad, Thompson, Scott M., and Shamsaei, Nima. "Laser Powder Bed Fusion of Ti-6Al-4V Parts: Thermal Modeling and Mechanical Implications." *International Journal of Machine Tools and Manufacture* Vol. 118–119 (2017): pp. 73–90.
- [17] Rai, Abha, Helmer, Harald, and Körner, Carolin. "Simulation of Grain Structure Evolution during

- Powder Bed Based Additive Manufacturing.” *Additive Manufacturing* Vol. 13 (2017): pp. 124–134.
- [18] Andreotta, Richard, Ladani, Leila, and Brindley, William. “Finite Element Simulation of Laser Additive Melting and Solidification of Inconel 718 with Experimentally Tested Thermal Properties.” *Finite Elements in Analysis and Design* Vol. 135 (2017): pp. 36–43.
- [19] Strano, Giovanni, Hao, Liang, Everson, Richard M., and Evans, Kenneth E. “Surface Roughness Analysis, Modelling and Prediction in Selective Laser Melting.” *Journal of Materials Processing Technology* Vol. 213 No. 4 (2013): pp. 589–597.
- [20] King, Wayne E., Anderson, Andrew T., Ferencz, Robert M., Hodge, Neil E., Kamath, Chandrika, Khairallah, Saad A., and Rubenchik, Alexander M. “Laser Powder Bed Fusion Additive Manufacturing of Metals; Physics, Computational, and Materials Challenges.” *Applied Physics Reviews* Vol. 2 No. 4 (2015): p. 041304.
- [21] Gao, Wei, Zhang, Yunbo, Ramanujan, Devarajan, Ramani, Karthik, Chen, Yong, Williams, Christopher B., Wang, Charlie C. L., Shin, Yung C., Zhang, Song, and Zavattieri, Pablo.D. “The Status, Challenges, and Future of Additive Manufacturing in Engineering.” *Computer-Aided Design* Vol. 69 (2015): pp. 65–89.
- [22] Choren, John Anthony, Heinrich, Stephen M., Silver-Thorn, M. Barbara. “Young’s Modulus and Volume Porosity Relationships for Additive Manufacturing Applications.” *Journal of Material Science* Vol. 48 No. 15 (2013): pp. 5103-5112.
- [23] Thompson, Scott M., Bian, Linkan, Shamsaei, Nima, and Yadollahi, Aref. “An Overview of Direct Laser Deposition for Additive Manufacturing; Part I: Transport Phenomena, Modeling and Diagnostics.” *Additive Manufacturing* Vol. 8 (2015): pp. 36–62.
- [24] Escobar-Palafox, Gustavo, Gault, Rosemary, and Ridgway, Keith. “Preliminary Empirical Models for Predicting Shrinkage, Part Geometry and Metallurgical Aspects of Ti-6Al-4V Shaped Metal Deposition Builds.” *IOP Conference Series: Materials Science and Engineering* Vol. 26 No. 1 (2011): p. 012002.
- [25] Spierings, A. B., Wegener, Konrad, and Levy, G. “Designing Material Properties Locally with Additive Manufacturing technology SLM.” *Solid Freeform Fabrication Symposium*. ETH-Zurich, Switzerland, August 6-8, 2012.
- [26] Collins, Linda M., Dziak, John J., and Li, Runze. “Design of Experiments with Multiple Independent Variables: A Resource Management Perspective on Complete and Reduced Factorial Designs.” *Psychological Methods* Vol. 14 No. 3 (2009): pp. 202–224.
- [27] Montgomery, Douglas C. *Design and Analysis of Experiments*. John Wiley & Sons, 2017.
- [28] Mahmoudi, Mohamad, Tapia, Gustavo, Karayagiz, Kubra, Franco, Brian, Ma, Ji, Arroyave, Raymundo, Karaman, Ibrahim, and Elwany, Alaa. “Multivariate Calibration and Experimental Validation of a 3D Finite Element Thermal Model for Laser Powder Bed Fusion Metal Additive Manufacturing.” *Integrated Materials and Manufacturing Innovation* Vol. 7 No. 3 (2018): pp. 116–135.
- [29] ASTM. “F2921 - Standard Terminology for Additive Manufacturing - Coordinate Systems and Test Methodologies.” (2012).
- [30] ASTM. “Standard Test Methods for Tension Testing of Metallic Materials.” (2009).
- [31] ASTM. “Standard Test Methods for Elevated Temperature Tension Tests of Metallic Materials.” (2016).
- [32] Akhavan Niaki, Farbod, Ulatan, Durul, and Mears, Laine. “Parameter Influence Under Uncertainty in End-Milling γ' -Strengthened Difficult-to-Machine Alloy.” *Journal of Manufacturing Science and Engineering* Vol. 138 (2016): pp. 061014+10.
- [33] Hoff, Peter D. *A First Course in Bayesian Statistical Methods*. Springer, New York, NY (2009).
- [34] Solonen, Antti. “Monte Carlo Methods in Parameter Estimation of Nonlinear Models.” MS Thesis. Lappeenranta University of Technology, Lappeenranta, Finland. 2006.